Journal of Innovative Optical Health Sciences
Vol. 1, No. 1 (2008) 95–106

World Scientific
www.worldscientific.com

RAMAN SPECTROSCOPY FOR *IN VIVO* TISSUE ANALYSIS AND DIAGNOSIS, FROM INSTRUMENT DEVELOPMENT TO CLINICAL APPLICATIONS

HAISHAN ZENG*, JIANHUA ZHAO, MICHAEL SHORT,
DAVID I. MCLEAN, STEPHEN LAM, ANNETTE MCWILLIAMS
and HARVEY LUI

Laboratory for Advanced Medical Photonics (LAMP)
Cancer Imaging Department
British Columbia Cancer Research Centre
675 West 10th Avenue
Vancouver, BC, V5Z 1L3, Canada

Photomedicine Institute
Department of Dermatology and Skin Science
University of British Columbia
and Vancouver Coastal Health Research Institute
835 West 10th Avenue
Vancouver, BC, V5Z 4E8, Canada
**hzeng@bccrc.ca*

Raman spectroscopy is a noninvasive, nondestructive analytical method capable of determining the biochemical constituents based on molecular vibrations. It does not require sample preparation or pretreatment. However, the use of Raman spectroscopy for *in vivo* clinical applications will depend on the feasibility of measuring Raman spectra in a relatively short time period (a few seconds). In this work, a fast dispersive-type near-infrared (NIR) Raman spectroscopy system and a skin Raman probe were developed to facilitate real-time, noninvasive, *in vivo* human skin measurements. Spectrograph image aberration was corrected by a parabolic-line fiber array, permitting complete CCD vertical binning, thereby yielding a 16-fold improvement in signal-to-noise ratio. Good quality *in vivo* skin NIR Raman spectra free of interference from fiber fluorescence and silica Raman scattering can be acquired within one second, which greatly facilitates practical noninvasive tissue characterization and clinical diagnosis. Currently, we are conducting a large clinical study of various skin diseases in order to develop Raman spectroscopy into a useful tool for non-invasive skin cancer detection. Intermediate data analysis results are presented. Recently, we have also successfully developed a technically more challenging endoscopic Laser-Raman probe for early lung cancer detection. Preliminary *in vivo* results from endoscopic lung Raman measurements are discussed.

Keywords: Rapid Raman system; *in vivo* skin Raman; *in vivo* lung Raman; endoscopic Raman probe; early cancer detection.

*Corresponding author.

1. Introduction

When monochromatic light strikes a sample, almost all the observed light is scattered elastically (Rayleigh scattering) with no change in energy (or frequency). A very small portion of the scattered light, ~ 1 in 10^{10}, is inelastically scattered (Raman scattering) with a corresponding change in frequency. The difference between the incident and scattered frequencies corresponds to an excitation of the molecular system, most often excitation of vibrational modes. By measuring the intensity of the scattered photons as a function of the frequency difference, a Raman spectrum is obtained. Raman peaks are typically narrow and in many cases can be attributed to the vibration of specific chemical bonds (or normal mode dominated by the vibration of a functional group) in a molecule. As such, it is a "fingerprint" for the presence of various molecular species and can be used for both qualitative identification and quantitative determination.[1]

Raman spectra have been observed from various biological tissues including brain, breast, bladder, colon, larynx, cervix, lung, and skin etc.[2–20] Identified Raman scatters in tissues include elastin, collagen, blood, lipid, tryptophan, tyrosine, carotenoid, myoglobin, nucleic acids etc. Most early studies obtained data from *ex vivo* tissue samples using Fourier-Transform (FT) Raman spectrometers. These data have demonstrated the great potential of Raman spectroscopy for disease diagnosis. Raman spectroscopy has also been used to monitor cutaneous drug delivery and pharmacokinetics during skin disease treatment.[21–23] It has been used to monitor blood analytes, e.g. glucose, lactic acid, and urea, in blood samples, and this kind of monitoring could potentially be carried out through trans-cutaneous Raman spectral measurements.[24–26] For all these applications to become practical, Raman measurements must be performed *in vivo* and in real-time. This is challenging because Raman signals are extremely weak. Only 10^{-10} of the incident light is Raman scattered. FT-Raman systems take up to half an hour to acquire a spectrum and are bulky and not portable, and therefore are of limited clinical utility.[3] Recently developed dispersive type Raman systems based on fiber optic light delivery and collection, compact diode lasers, and high efficiency spectrograph-detector combinations, have shorten the *in vivo* tissue Raman spectral measurement time to minutes or sub-minutes.[27–29]

Very recently, several groups including our laboratory have further optimized the Raman probe design and improved the Raman signal collection efficiency.[14,30,31] Integration of these probes with state-of-the-art dispersive type Raman systems have led to successful *in vivo* real-time Raman measurements on various organs (e.g. the cervix, the gastrointestinal (GI) tract, the skin, and the lung[14,29,30,32–34]). Some of these systems are capable of acquire an *in vivo* Raman spectra within seconds or sub-seconds, paved the way for clinical applications. In this paper, we will summarize our experiences on the development of a rapid Raman system and its applications in skin cancer and lung cancer detection.

2. Instrument Development

2.1. *System configurations*

We first developed a rapid Raman system for *in vivo* skin applications.[14,35] Figure 1 shows the block diagram of the system. It consists of a stabilized diode laser (785 nm, 300 mW; Model 8530, SDL), a transmissive imaging spectrograph (HoloSpec-f/2.2-NIR, Kaiser), a NIR-optimized, back-illuminated, deep-depletion, CCD detector (LN/CCD-1024EHRB, Princeton Instruments), and a specially designed Raman probe. The laser is coupled to the Raman probe via a 100 μm core-diameter fiber. Tissue-scattered Raman photons are collected from the probe by a fiber bundle and fed into the spectrograph, where the photons are dispersed onto the CCD array detector by a volume-phase technology holographic grating. A PC computer controls the CCD detector and the spectral data acquisition, processing, and display. The CCD, with enhanced quantum efficiency and reduced etaloning in the NIR (quantum efficiency, $> 75\%$ at 900 nm), was liquid-nitrogen cooled, and its S/N ratio was readout noise limited when weak Raman signals were acquired. The CCD consisted of 1024×256 pixels ($27\,\mu\text{m} \times 27\,\mu\text{m}$) and allowed vertical binning for improved detection sensitivity. The spectrograph's f-number of 2.2 very well matched the N.A. of the fiber bundle (0.22), which in turn provided five times better throughput than traditional f/4, quarter-meter imaging Czerny–Turner spectrographs used in conventional dispersive Raman systems. The whole system was packed onto a movable cart for outpatient clinical data acquisition.

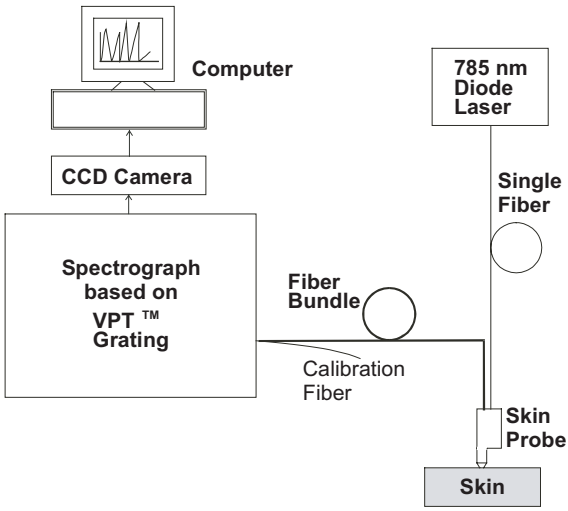

Fig. 1. Block diagram of the rapid Raman system for *in vivo* skin measurements.

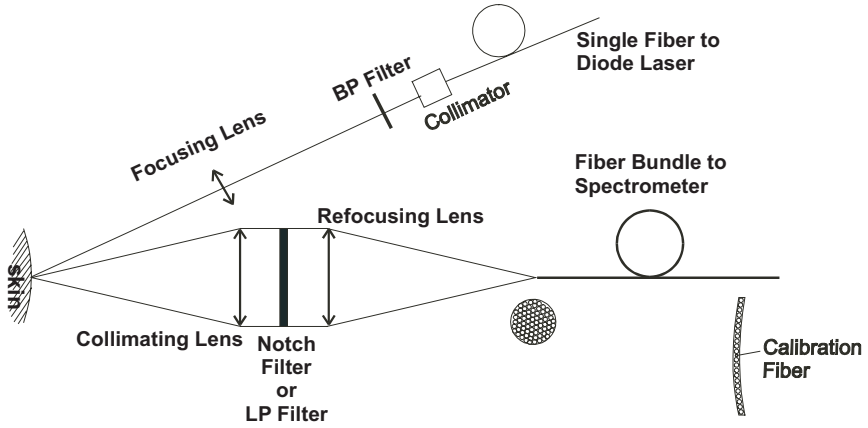

Fig. 2. Optical configuration of the skin Raman probe.

2.2. *Skin Raman probe*

We designed the Raman probe to maximize the collection of tissue Raman signals while reducing the interference of Rayleigh-scattered light, fiber fluorescence, and silica Raman signals.[14,35] The probe consisted of two arms, as shown in Fig. 2. A 0.5-inch diameter optics illumination arm that incorporated a collimating lens, a bandpass (BP) filter (785 ± 2.5 nm), and a focusing lens delivered the laser light onto the skin surface, with a spot size of about 3.5 mm. A 1-inch diameter optics collection arm with collimating and refocusing lenses and a holographic notch plus filter (optical density > 6.0 at 785 nm; Kaiser) was used for collecting Raman emissions. A high performance long pass (LP) filter can also be used to replace the notch filter (e.g. model LP-01-785RU-25, Semrock, Rochester, NY). The collimating lens was positioned so that its focal point was located at the skin surface, leading to a collimated beam between the two lenses. The notch filter or LP filter between the two lenses blocked the backscattered laser light and pass the frequency-shifted Raman signal. A refocusing lens then focused the filtered beam onto the circular end of the fiber bundle. The collection arm was perpendicular to the skin surface, and we placed the illumination arm at a 40° degree angle to avoid collection of specularly reflected laser light. We mounted all optical components in a rigid metal case to keep them in the desired positions.

To enhance the detection of the inherently weak Raman signals, we packed as many fibers into the fiber bundle as allowed by the CCD height (6.9 mm). The fiber bundle consisted of more than fifty 100 μm fibers arranged in a circular shape at the input end of the probe and a linear array at the output end that was connected to the spectrograph's entrance. Another 50 μm fiber was placed at the center of the output linear array and split out of the bundle for wavelength calibration. At the circular end the fibers were packed into a 1.3 to 1.6 mm diameter area, which also defined the measurement spot size at the skin surface.

It is well known that the image of a straight slit through any spectrograph utilizing a plane grating has a curved shape that is usually parabolic. This image aberration causes two problems for hardware binning of CCD columns: (1) It decreases the spectral resolution and (2) it decreases the S/N ratio that is achievable otherwise. It also causes problems with wavelength calibration. Hardware binning is CCD binning performed before signal readout by the preamplifier. For signal levels that are readout-noise limited, for instance, for weak Raman signal measurements, hardware binning improves the S/N ratio linearly with the number of pixels grouped together. Binning can also be done by use of software after the signal is read out. However, software binning improves the S/N ratio by only as much as the square root of the number of pixels added together. Hence, complete hardware binning of the entire vertical line is preferable for maximizing the S/N ratio. We conceived a simple but novel solution for dealing with this image aberration. As shown in Fig. 2, we aligned the 50+ fibers of the fiber bundle at the spectrograph's end along a curve formed by laser drilling of a stainless-steel cylinder piece,[36] the shape of which corresponded directly to the horizontal displacement caused by the spectrograph image aberration but in the reverse orientation. With this specific fiber arrangement effective image-aberration correction was achieved, allowed us to completely bin the entire CCD vertical line (256 pixels) without losing resolution and reducing the S/N ratio. The S/N ratio improvement that we achieve with our system could be up to a maximum value of $256/\sqrt{256} = 16$ times that of the software binning.

2.3. *Endoscopy Raman probe*

We have successfully developed an endoscopic laser-Raman probe for real-time *in vivo* lung Raman measurements.[37] The key specifications of the endoscopic laser-Raman probe are (1) small enough to pass through the bronchoscope instrument channel (2.2 mm size), (2) incorporating proper filtering mechanism to minimize or eliminate the background Raman and fluorescence signals generated from the fiber itself, and (3) able to collect enough signal so that a Raman spectrum can be acquired in seconds or sub-seconds. To preserve the high S/N ratio advantage of our skin Raman probe, we employed a two-step filtering strategy for the endoscopic Raman probe: (1) first order filtering at the tip of the fiber bundle and (2) high performance filtering at the entrance point of the instrument channel of the endoscope. Figure 3 shows the schematics of the probe we built. It consists of a probing fiber bundle assembly, a filter adapter, an illumination fiber, and a round to parabolic linear array fiber bundle. The 785 nm laser light is focused into the illumination fiber, which is connected to the filter adapter close to the instrument channel entrance. A high performance BP (band pass) filter (785 ± 2.5 nm) passes through the laser light and filters out the background Raman and fluorescence signals generated inside the illumination fiber between the laser and the filter adapter. The filtered laser light is refocused into the illumination fiber in the probing fiber

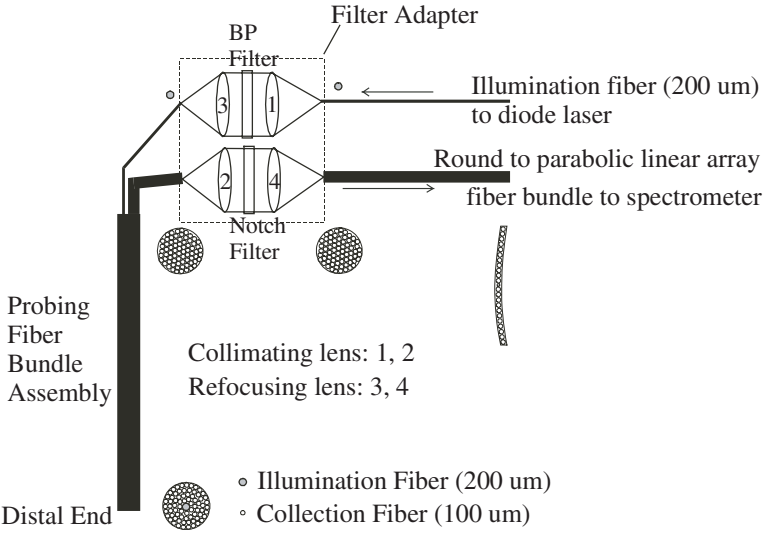

Fig. 3. Schematic diagram of the endoscopic laser-Raman probe.

bundle assembly. Because this part of the illumination fiber is short, the generated background Raman and fluorescence is small. Nevertheless, the distal end of the illumination fiber is coated with a SP (short pass) filter to further reduce these background signals. The induced Raman signal from the tissue is picked up by collection fibers in the probing fiber bundle assembly. LP filter coatings are applied to these fibers to block the back-scattered laser light from entering the probe. At the proximal end of the probing fiber bundle assembly, these collection fibers are packed into a round bundle and connected to the filter adapter. A notch filter ($OD > 6$ at 785 nm, Kaiser) is used to further block the laser wavelengths and allow the Raman signals to pass through. The Raman signals are refocused by lens 4 into the round to parabolic linear array fiber bundle. At the entrance of the spectrometer, these collection fibers are aligned along a parabolic line to correct for image aberration of the spectrograph to achieve better spectral resolution and higher S/N ratio in a fashion similar to our skin Raman probe (Fig. 2). In the lung Raman system, the endoscopic laser-Raman probe replaces the skin Raman probe of the skin Raman system as shown in Figs. 1 and 2.

2.4. *System calibration*

With a LF grating, the system covered the low frequency fingerprint spectral range up to 1800 cm^{-1}. While using a HF grating, the system is capable of measuring Raman spectra from 1500 cm^{-1} to 3500 cm^{-1}. Raman frequencies were calibrated with cyclohexane, acetone, and barium sulfate to an accuracy of $\pm 2\,cm^{-1}$, and the spectral resolution was 8 cm^{-1}. All spectra acquired were corrected for the

spectral sensitivity of the system by use of a standard lamp (RS-10, EG&G Gamma Scientific).

2.5. *Data processing*

One of the major challenges for biomedical Raman spectroscopy is the removal of intrinsic autofluorescence background signals, which are usually a few orders of magnitude stronger than those arising from Raman scattering. A number of methods have been proposed for fluorescence background removal including excitation wavelength shifting, Fourier transformation, time gating, and simple or modified polynomial fitting. The single polynomial and the modified multi-polynomial fitting methods are relatively simple and effective, and thus widely used in biological applications. However, their performance in real-time *in vivo* applications and low signal-to-noise ratio environments is suboptimal. We have developed an

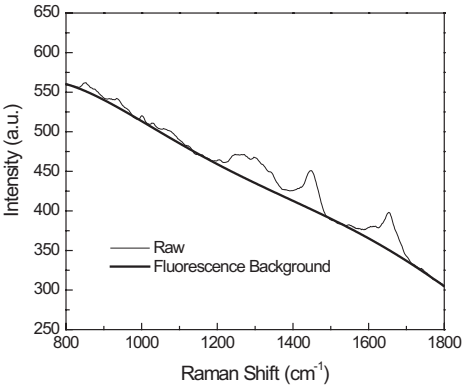

(a)

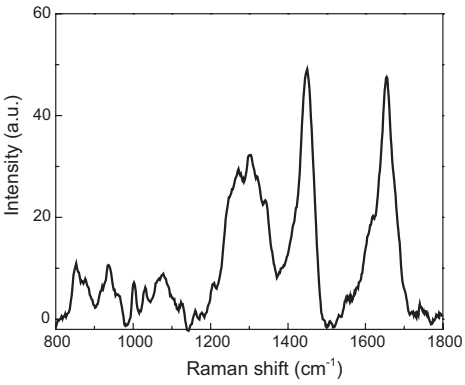

(b)

Fig. 4. Fluorescence background removal from a volunteer's palm skin.

improved automated algorithm[38] for fluorescence removal based on modified multi-polynomial fitting, but with the addition of (1) a peak-removal procedure during the first iteration, and (2) a statistical method to account for signal noise effects. Experimental results demonstrate that this approach improves the automated rejection of the fluorescence background during real-time Raman spectroscopy and for *in vivo* measurements characterized by low signal-to-noise ratios. Figure 4(a) shows the raw data and the fitted fluorescence background, while Fig. 4(b) shows the pure Raman signal after subtracting the fitted fluorescence background from the raw data. Details of this algorithm can be found in our reference[38] and a computer code will soon be posted on our website (http://www.bccrc.ca/ci/people_hzeng.html).

2.6. *Software*

We have developed an Labview (drivers from R Cubed Software, Lawrenceville, NJ) based system software for both data acquisition and analysis including CCD dark-noise subtraction, wavelength calibration, spectral response calibration, intensity calibration, signal saturation detection, cosmic ray rejection, fluorescence background removal, and composition modeling. Details can be found in our reference.[35]

3. Clinical Applications

Using the two rapid Raman systems, we have conducted various *in vivo* clinical applications as summarized below.

3.1. *Raman spectroscopy of normal skin*

We have measured *in vivo* Raman spectra of normal skin on 25 different body sites of 30 healthy volunteers.[39] Distinct Raman peaks in the 800–1800 cm^{-1} range can be discerned clearly from various skin sites of the body. Information about chemical compositions of the skin can be evaluated quickly and non-invasively. We found that within the same subject, skin Raman signals are significantly different for different body sites. However, the inter-subject differences of skin Raman signals for a given body site are relatively small.

3.2. *Raman spectroscopy of* in vivo *cutaneous melanin*

We successfully acquire the *in vivo* Raman spectrum of melanin from human skin using the rapid near-infrared (NIR) Raman spectrometer as shown in Figs. 1 and 2.[32] The Raman signals of *in vivo* cutaneous melanin are similar to those observed from natural and synthetic eumelanins. The melanin Raman spectrum is dominated by two intense and broad peaks at about 1580 and 1380 cm^{-1}, which can be interpreted as originating from the in-plane stretching of the aromatic rings and the linear stretching of the C–C bonds within the rings, along with some

contributions from the C–H vibrations in the methyl and methylene groups. Variations in the peak frequencies and bandwidths of these two Raman signals due to differing biological environments have been observed in melanin from different sources.

3.3. *Raman spectroscopy for non-invasive skin cancer detection*

Currently, we are conducting a large clinical study of various skin diseases in order to develop Raman spectroscopy into a useful tool for non-invasive skin cancer detection. We have conducted an intermediate data analysis based on data from 274 lesions including skin cancers (melanoma — 31 cases, basal cell carcinoma — 18 cases, and squamous cell carcinoma — 39 cases), precancerous lesion (actinic keratosis — 20 cases), and benign lesions such as seborrheic keratosis (48 cases), and various nevi (atypical nevus — 32 cases, compound nevus — 20 cases, intradermal nevus — 25 cases, jounctional nevus — 23 cases, nevus of Ota — 10 cases, and blue nevus — 8 cases). We used partial least square (PLS) regression of the measured Raman spectra to derive the biochemical constituents in each lesion. Linear discriminant analysis (LDA) of the derived molecular quantities is then used to classify various skin diseases. Our results showed that malignant melanoma can be differentiated from other pigmented skin lesions with a diagnostic sensitivity of 100% and specificity of 70%, while precancerous and cancerous lesions can be differentiated from benign lesions with a sensitivity of 90% and a specificity of 75%. This is very encouraging for Raman applications in clinical non-invasive skin cancer detection.

3.4. *Raman spectroscopy for early lung cancer detection*

Recently, we have also successfully developed a technically more challenging endoscopic Laser-Raman probe (Fig. 3) for early lung cancer detection.[37] We successfully acquired for the first time *in vivo* lung Raman spectra. The spectral measurement can be performed in real-time with 1–2 second integration times. We found that strong autofluorescence of the lung in the low frequency range rendered the extraction of Raman signals in this emission range unreliable. However, reliable *in vivo* lung Raman spectra could be obtained using the high frequency emission range, and these showed significant spectral differences between benign and malignant tissue types. These preliminary findings present great potential for lung tissue characterization at the molecular level and for improving the early detection of lung cancers. Large scale clinical study is under way.

4. Concluding Remarks

After almost 10 years of effort, we have successfully developed a rapid dispersive type Raman spectroscopy system and probes for non-invasive skin cancer detection and for improving endoscopic lung cancer detection. The system can acquire

a Raman spectrum from skin *in vivo* in sub-seconds and from lung *in vivo* in seconds. Information about chemical composition of the skin and lung tissue can be evaluated quickly and non-invasively (skin) or minimal invasively (lung). Within the same subject, skin Raman signals are significantly different for different body sites. However, the inter-subject differences of skin Raman signals for a given body site are relatively small. Clinical data collection is ongoing in both skin and lung in our institute. Intermediate data analysis of 274 skin lesions demonstrated that Raman spectroscopy can be used to differentiate skin cancers from benign lesions with very good sensitivity and specificity. *In vivo* NIR Raman spectroscopy presents significant potential for non-invasive tissue analysis and for early cancer detection.

Acknowledgments

This work is supported by the National Cancer Institute of Canada with funds from the Canadian Cancer Society, the Canadian Institutes of Health Research (Grant No. PPP-79109 and MOP-85011), the Canadian Dermatology Foundation, the VGH & UBC Hospital Foundation In It for Life Fund, and the BC Hydro Employees Community Services Fund. We would like to acknowledgment the contributions of our previous group members: Dr. Zhiwei Huang, Dr. Iltefat Hamzavi, Dr. Abdulmajeed Alajlan, Dr. Hana Alkhayat, Dr. Ahmad Al Robaee, and Miss Michelle Zeng. We also thank Mr. Wei Zhang for his technical assistance.

References

1. J. G. Grasselli and B. J. Bulkin, *Analytical Raman Spectroscopy, Chemical Analysis Series Vol. 114* (John Wiley, New York, 1991).
2. Y. Ozaki, "Medical application of Raman spectroscopy," *Appl. Spectr. Rev.* **24**, 259 (1988).
3. R. Manoharan, Y. Wang and M. S. Feld, "Histochemical analysis of biological tissues using Raman spectroscopy," *Spectro. Acta Part A* **52**, 215 (1996).
4. A. Mahadevan-Jansen and R. Richards-Kortum, "Raman spectroscopy for the detection of cancers and precancers," *J. Biomed. Opt.* **1**, 31 (1996).
5. C. J. Frank, R. L. McCreery and D. C. Redd, "Raman spectroscopy of normal and diseased human breast tissues," *Anal. Chem.* **67**, 777 (1995).
6. R. Manoharan, K. Shafer, L. Perelman, J. Wu, K. Chen, G. Deinum, M. Fitzmaurice, J. Myles, J. Crowe, R. Dasari and M. S. Feld, "Raman spectroscopy and fluorescence photon migration for breast cancer diagnosis and imaging," *Photochem. Photobiol.* **67**, 15 (1998).
7. B. Schrader, S. Keller, T. Loechte, S. Fendel, D. S. Moore, A. Simon and J. Sawatzki, "NIR FT Raman spectroscopy in medical diagnosis," *J Mol. Struct.* **348**, 293 (1995).
8. E. E. Lawson, B. W. Barry, A. C. Williams and H. G. M. Edwards, "Biomedical applications of Raman spectroscopy," *J Raman Spectrosc.* **28**, 111 (1997).
9. C. H. Liu, B. B. Das, W. L. Glassman, G. C. Tang, K. M. Yoo, H. R. Zhu, D. L. Akins, S. S. Lubicz, J. Cleary, R. Prudente, E. Celmer, A. Caron and R. R. Alfano, "Raman, fluorescence and time-resolved light scattering as optical diagnostic techniques to separate diseased and normal biomedical media," *J. Photochem. Photobiol. B:Biol.* **16**, 187 (1992).

10. A. Mahadevan-Jansen, M. F. Mitchell, N. Ramanujam, A. Malpica, S. Thomsen, U. Utzinger and R. Richards-Kortum, "Near-infrared Raman spectroscopy for *in vitro* detection of cervical precancers," *Photochem. Photobiol.* **68**, 123 (1998).
11. A. Mizuno, H. Kitajima, K. Kawauchi, S. Muraishi and Y. Ozaki, "Near-infrared Fourier transform Raman spectroscopic study of human brain tissues and tumors," *J. Raman Spectrosc.* **25**, 25 (1994).
12. N. Stone, P. Stavroulaki, C. Kendall, M. Birchall and H. Barr, "Raman spectroscopy for early detection of laryngeal malignancy: preliminary results," *The Laryngoscope* **110**, 1756 (2000).
13. R. R. Alfano, C. H. Liu, W. L. Sha, D. Zhu, L. Akins, J. Cleary, R. Prudente and E. Cellmer, "Human breast tissues studied by IR Fourier transform Raman spectroscopy," *Lasers Life Sci.* **4**, 23 (1991).
14. Z. Huang, H. Zeng, I. Hamzavi, D. I. McLean and H. Lui, "A rapid near-infrared Raman spectroscopy system for real-time *in vivo* skin measurements," *Optics Letters* **26**, 1782 (2001).
15. D. P. Lau, Z. Huang, H. Lui, C. S. Man, K. Berean, M. D. Morrison and H. Zeng, "Raman spectroscopy for optical diagnosis in normal and cancerous tissue of the nasopharynx — preliminary findings," *Lasers in Medicine and Surgery* **32**, 210 (2003).
16. Z. Huang, A. McWilliams, S. Lam, J. English, D. I. McLean, H. Lui and H. Zeng, "Effect of formalin fixation on the near-infrared Raman spectroscopy of human bronchial tissues," *Intl. J. Oncology* **23**, 649 (2003).
17. Z. Huang, A. McWilliams, H. Lui, D. I. McLean, S. Lam and H. Zeng, "Near-infrared raman spectroscopy for optical diagnosis of lung cancer," *Intl. J. Cancer* **107**, 1047 (2003).
18. Z. Huang, H. Lui, D. I. McLean, M. Korbelik and H. Zeng, "Raman spectroscopy in combination with background near-infrared autofluorescence enhances the *in vivo* assessment of malignant tissues," *Photochem. and Photobiol.* **81**, 1219 (2005).
19. D. P. Lau, Z. Huang, H. Lui, D. W. Anderson, K. Berean, M. D. Morrison, S. Liang and H. Zeng, "Raman spectroscopy for optical diagnosis in the larynx — preliminary findings," *Lasers in Surgery and Medicine* **37**, 192 (2005).
20. M. A. Short, H. Lui, D. I. McLean, H. Zeng, A. Alajlan and M. X. Chen, "Demonstrating changes in nuclei and peritumoral collagen within nodular basal cell carcinomas via confocal micro-Raman spectroscopy," *J. Biomedical Optics* **11**, 034004 (2006).
21. K. U. Schallreuter, "Successful treatment of oxidative stress in vitiligo," *Skin Pharmacol Appl. Skin Physiol.* **12**, 132–138 (1999).
22. E. E. Lawson, H. G. Edwards, B. W. Barry and A. C. Williams, "Interaction of salicylic acid with verrucae assessed by FT-Raman spectroscopy," *J. Drug Target* **5**, 343 (1998).
23. K. U. Schallreuter, M. Zschiesche, J. Moore, A. Panske, N. A. Hibberts, F. H. Herrmann, H. R. Metelmannn and J. Sawatzki, "*In vivo* evidence for compromised phenylalanine metabolism in vitiligo," *Biochem. Biophys Res. Commun.* **243**, 395 (1998).
24. A. J. Berger, I. Itzkan and M. S. Feld, "Feasibility of measuring blood glucose concentration by near-infrared Raman spectroscopy," *Spectrochim Acta. A. Mol. Biomol. Spectrosc.* **53A**, 287 (1997).
25. M. J. Jr Goetz, G. L. Cote, R. Erckens, W. March and M. Motamedi, "Application of a multivariate technique to Raman spectra for quantification of body chemicals," *IEEE Trans. Biomed. Eng.* **42**, 728 (1995).
26. A. J. Berger, T. W. Koo, I. Itzkan, G. Horowitz and M. S. Feld, "Multicomponent blood analysis by near-infrared Raman spectroscopy," *Appl. Opt.* **38**, 2916 (1999).

27. J. J. Baraga, M. S. Feld and R. P. Rava, "Rapid near-infrared Raman spectroscopy of human tissue with a spectrograph and CCD detector," *Appl. Spectro.* **46**, 187 (1992).
28. J. R. Kramer, J. F. Brennan, T. J. Romer, Y. Wang, R. R. Dasari and M. S. Feld, "Spectral diagnosis of human coronary artery: a clinical system for real time analysis," *SPIE Proc.* **2395**, 376 (1995).
29. A. Mahadevan-Jansen, M. F. Mitchell, N. Ramanujam, U. Utzinger and R. Richards-Kortum, "Development of a fiber optic probe to measure NIR Raman spectra of cervical tissue *in vivo*," *Photochem. Photobiol.* **68**, 427 (1998).
30. M. G. Shim, L. K. S. Wong, N. E. Marcon and B. C. Wilson, "*In vivo* near-infrared Raman spectroscopy: demonstration of feasibility during clinical gastrointestinal endoscopy," *Photochem. Photobiol.* **72**, 146 (2000).
31. J. T. Motz, M. Hunter, L. H. Galindo, J. A. Gardecki, J. R. Kramer, R. R. Dasari and M. S. Feld, "Optical fiber probe for biomedical Raman spectroscopy," *Appl. Opt.* **43**, 542 (2004).
32. Z. Huang, H. Lui, M. X. K. Chen, D. I. McLean and H. Zeng, "Raman spectroscopy of *in vivo* cutaneous melanin," *J. Biomedical Optics* **9**, 1198 (2004).
33. U. Utzinger, D. L. Heintzelman, A. Mahadevan-Jansen, A. Malpica, M. Follen and R. Richards-Kortum, "Near-infrared Raman spectroscopy for *in vivo* detection of cervical precancers," *Appl. Spectrosc.* **55**, 955 (2001).
34. A. Molckovsky, L. M. W. K. Song, M. G. Shim, N. E. Marcon and B. C. Wilson, "Diagnostic potential of near-infrared Raman spectroscopy in the colon: differentiating adenomatous from hyperplastic polyps," *Gastrointestinal Endoscopy* **57**, 396 (2003).
35. J. Zhao, H. Lui, D. I. McLean and H. Zeng, "Integrated real-time Raman system for clinical *in vivo* skin analysis," *Skin Research and Technology*, March 18, 2008, doi #: 10.1111/j.1600-0846.2008.00321.
36. H. Zeng, "Apparatus and methods relating to high speed Raman spectroscopy," United States Patent #6,486,948, November 26, 2002.
37. M. Short, S. Lam, A. McWilliams, J. Zhao, H. Lui and H. Zeng, "Development and preliminary results of an endoscopic Raman probe for potential *in vivo* diagnosis of lung cancers," *Optics Letters* **33**, 711 (2008).
38. J. Zhao, H. Lui, D. I. McLean and H. Zeng, "Automated autofluorescence background subtraction algorithm for biomedical Raman spectroscopy," *Applied Spectroscopy* **61**, 1225 (2007).
39. Z. Huang, H. Zeng, I. Hamzavi, D. I. McLean and H. Lui, "Evaluation of variations of biomolecular constituents in human skin *in vivo* by near-infrared Raman spectroscopy," *SPIE Proc.* **4597**, 109 (2001).